International Journal of Thermophysics, Vol. 9, No. 5, 1988

Computer Simulation of Fluids Using Axisymmetric Molecules[1]

S. Gupta,[2] W. B. Sediawan,[2] C. P. Williams,[2,3] and E. McLaughlin[2]

Molecular dynamics simulations have been performed using the Gaussian overlap potential in order to develop and test thermodynamic property predictive methods and to investigate the possibility of modeling real fluids as well. A first-order anisotropic reference-based perturbation theory and a temperature-dependent sphericalized potential have been tested and these methods are shown to work well, qualitatively for the original Gaussian overlap potential and qualitatively as well as quantitatively for the modified Gaussian overlap potential. It is also shown that the modified Gaussian overlap potential with the quadrupole moment works well for modeling benzene. Future possibilities are also discussed.

KEY WORDS: free energy; intermolecular forces; liquids; molecular dynamics; statistical mechanics; thermodynamics.

1. INTRODUCTION

Site–site interaction models, in which the interaction sites are usually modeled as spheres, have been popular in the modeling of fluids of non-spherical models. However, such models can become not only computationally difficult [1, 2] but also less convenient for theoretical developments for the case of complex molecules requiring several sites [3]. An alternative is to use pseudoatomic models [1], of which the Gaussian overlap potential [4, 5] is of particular interest. Through this model, both prolate and oblate shapes of molecules can be represented as axially symmetric molecules [3]. This allows possible alternatives to the use of the

---

[1] Paper presented at the Tenth Symposium on Thermophysical Properties, June 20–23, 1988, Gaithersburg, Maryland, U.S.A.

[2] Department of Chemical Engineering, Louisiana State University, Baton Rouge, Louisiana 70803-7303, U.S.A.

[3] Present address: Royal Dutch Shell Laboratory, Amsterdam, The Netherlands.

0195-928X/88/0900-0781$06.00/0

spherical site–site interactions not only for molecules such as N_2 and O_2, which are traditionally modeled as linear molecules, but also for molecules with cyclic and aromatic rings. Further, this model can be combined with the site–site model to represent even more complex molecules such as naphthalene and ethylbenzene [4].

In the past, the Gaussian overlap potential has been used in simulations involving liquid crystal studies [6], development of a non-spherical reference-based perturbation theory [2], and studies of liquid structure as well as comparisons with the experimental data [7, 8]. All these papers clearly indicate the need for more systematic simulation studies and this paper summarizes our recent simulation results [9–11] using the Gaussian overlap potential.

2. POTENTIAL MODEL DEVELOPMENT

For a pair of molecules, with orientations ω_1 and ω_2 with respect to vector $\mathbf{r}$ along the molecular centers of mass, the original Gaussian overlap pair potential of Berne and Pechukas [4] is given by

$$U(r\omega_1\omega_2) = 4\varepsilon(\omega_1\omega_2)\left[\left(\frac{\sigma(\omega_1\omega_2)}{r}\right)^{12} - \left(\frac{\sigma(\omega_1\omega_2)}{r}\right)^{6}\right] \tag{1}$$

with

$$\varepsilon(\omega_1\omega_2) = \varepsilon_0[1-\chi^2(\mathbf{v}_1\cdot\mathbf{v}_2)^2]^{-1/2} \tag{2}$$

and

$$\sigma(\omega_1\omega_2) = \sigma_0\left[1-\frac{\chi}{2}\left(\frac{(\mathbf{r}\cdot\mathbf{v}_1+\mathbf{r}\cdot\mathbf{v}_2)^2}{1+\chi(\mathbf{v}_1\cdot\mathbf{v}_2)} + \frac{(\mathbf{r}\cdot\mathbf{v}_1-\mathbf{r}\cdot\mathbf{v}_2)^2}{1-\chi(\mathbf{v}_1\cdot\mathbf{v}_2)}\right)\right]^{-1/2} \tag{3}$$

Here $\mathbf{v}_1$ and $\mathbf{v}_2$ are the unit vectors along the symmetry axes of these molecules, ε_0 and σ_0 are the potential parameters, and χ is the anisotropy parameter given by

$$\chi = (\kappa^2-1)/(\kappa^2+1) \tag{4}$$

where κ is the length-to-breadth ratio of these molecules such that $\kappa > 1$ for prolate molecules and $\kappa < 1$ for oblate molecules. Equations (1)–(4) define the pair potential between two identical axially symmetric molecules whose shapes are closely ellipsoidal [3]. Kabadi and Steele [7] recognized that the orientation dependence of $\varepsilon(\omega_1\omega_2)$ as given by Eq. (2) is weak and simply used

$$\varepsilon(\omega_1\omega_2) = \varepsilon_0 \tag{5}$$

This potential, Eqs. (1), (3), and (5), is referred to as the GOCE potential and produces results for thermodynamic properties [9] close to those of the original potential of Berne and Pechukas [4]. This model provides for a strong angle dependence of the width of the attractive well and this, besides a constant ε, is the main deficiency of this model compared with the site–site potentials.

Gay and Berne [5] have attempted to improve the Gaussian overlap potential by modifying Eqs. (1) and (3). We use a simplified version of their potential where the r dependence is given by

$$U(r\omega_1\omega_2) = 4\varepsilon(\omega_1\omega_2)\left[\left(\frac{d_w}{r-\sigma(\omega_1\omega_2)+d_w}\right)^{12} - \left(\frac{d_w}{r-\sigma(\omega_1\omega_1)+d_w}\right)^{6}\right] \tag{6}$$

The above form of potential leads to a nearly constant well width which is further controlled by a parameter d_w, introduced by Kabadi [8], such that $d_w = 1$ for prolate and $\approx\kappa$ for oblate molecules. The equation for $\sigma(\omega_1\omega_2)$ is still given by Eq. (3) and this has recently been shown to be a reasonable representation of the ellipsoids of revolution [3]. The orientation dependence of $\varepsilon(\omega_1\omega_2)$ has been modified according to

$$\varepsilon(\omega_1\omega_2) = \varepsilon_0[1-\chi^2(\mathbf{v}_1\cdot\mathbf{v}_2)^2]^{1/2}/[\sigma(\omega_1\omega_2)/\sigma_0]^2 \tag{7}$$

We refer to this model, Eqs. (3), (6), and (7), as the GOBG potential. This model compares well with the equivalent site–site models and only some minor problems remain [5, 11].

Both the GOCE and the GOBG models discussed here are suitable for calculations of thermophysical properties through molecular dynamics and Monte Carlo simulations. Not only is the evaluation of the potential energy straightforward, for known $\mathbf{r}$, $\mathbf{v}_1$, and $\mathbf{v}_2$, but also analytical expressions for force and torque can be obtained through simple mathematical manipulations [12]. We have performed NVT molecular dynamics simulations using systems of 256 molecules for the results discussed in the next section. More details can be found elsewhere [9–11].

3. SIMULATION AND THEORY

The thermodynamic perturbation theory of Fischer [13], originally developed for site–site models, has been easily adapted for the Gaussian overlap potential. The full intermolecular pair potential is divided into two parts: a "repulsive" reference part, $U_0(r\omega_1\omega_2)$, and an "attractive" perturbation part, $U_1(r\omega_1\omega_2)$, according to Mo and Gubbins [14]

$$\begin{aligned} U_0(r\omega_1\omega_2) &= U(r\omega_1\omega_2) - U_{\min}(\omega_1\omega_2), && r < r_{\min}(\omega_1\omega_2) \\ &= 0, && r > r_{\min}(\omega_1\omega_2) \end{aligned} \tag{8}$$

and

$$\begin{aligned} U_1(r\omega_1\omega_2) &= U_{\min}(\omega_1\omega_2), & r < r_{\min}(\omega_1\omega_2) \\ &= U(r\omega_1\omega_2), & r > r_{\min}(\omega_1\omega_2) \end{aligned} \tag{9}$$

where $r_{\min}$ is the r location of the attractive minimum of the full pair potential, $U(r\omega_1\omega_2)$, for a given ω_1 and ω_2, and $U_{\min}(\omega_1\omega_2)$ is the value of the potential at this minimum.

The perturbation expansion of Zwanzig can then be applied to obtain the residual Helmholtz free energy [1]

$$A = A_0 + A_1 + \cdots \tag{10}$$

where A_0 is the residual Helmholtz free energy of the reference fluid and is taken to be that of a hard ellipsoid (HE) having the same κ, with the size given by the numerical solution of

$$\int \hat{y}(r)\{\langle\exp[-\beta U_0(r\omega_1\omega_2)]\rangle - \langle\exp(-\beta U_{\mathrm{HE}})\rangle\}\, d\mathbf{r} = 0 \tag{11}$$

Here $\beta = 1/kT$ and $\hat{y}(r)$ is the background correlation function of the reference fluid [9, 10, 13]. The angle brackets represent ω_1 and ω_2. The first-order term, A_1, can be obtained from

$$A_1 = \frac{N\rho}{2} \int \langle U_1(r\omega_1\omega_2)\exp[-\beta U_0(r\omega_1\omega_2)]\rangle\, \hat{y}(r)\, d\mathbf{r} \tag{12}$$

Here we have used only the first-order perturbation expansion.

Recently, there has been some interest in using angle-averaged potentials [15–18] for predicting thermodynamic properties of fluids modeled with anisotropic potentials. Of special interest is the idea of MacGowan [19] and here we have followed similarly. In our case we divide the potential according to a Barker–Henderson-type split [20] in a manner similar to that of Mo and Gubbins [14]

$$\begin{aligned} U_0(r\omega_1\omega_2) &= U(r\omega_1\omega_2), & \text{if} \quad U(r\omega_1\omega_2) > 0 \\ &= 0, & \text{otherwise} \end{aligned} \tag{13}$$

and

$$\begin{aligned} U_1(r\omega_1\omega_2) &= U(r\omega_1\omega_2), & \text{if} \quad U(r\omega_1\omega_2) < 0 \\ &= 0, & \text{otherwise} \end{aligned} \tag{14}$$

This type of split is chosen since it applies to polar molecules also. These two parts are separately sphericalized using a Boltzmann angle-averaging procedure and then recombined such that

$$\exp(-\beta\phi) = \langle \exp[-\beta U_0(r\omega_1\omega_2)] \rangle \cdot \langle \exp[-\beta U_1(r\omega_1\omega_2)] \rangle \quad (15)$$

Thermodynamic properties of the fluid modeled by the sphericalized potential, ϕ, can then be easily obtained [15–19] and we have used a simplified form of Fischer's theory [13] for this purpose. We note that this form of the sphericalized potential is temperature dependent.

Systematic molecular dynamics simulations have been performed to obtain the residual Helmholtz free energy and these are compared with the predictions from perturbation theory and the sphericalized potential method for the GOCE model with $\kappa = 0.50$, 1.30, and 1.55 [9]. Figure 1 shows one such comparison for the case of $\kappa = 0.50$. The two methods are in qualitative agreement with simulation, with the deviations getting larger with increasing density or decreasing temperature. The sphericalized potential method is slightly better than perturbation theory at higher densities and lower temperatures. Similar behavior has also been found for other molecular shapes [9]. A comparison of the pressure shows the sphericalized potential method to be better than perturbation theory, however, both these methods underpredict the potential energy when compared with simulation [9]. We note that our observations are similar to those Monson and Gubbins [2] for the original potential of Berne and Pechukas [4].

We have performed simulations using the reference potential of Eq. (8) for the GOCE model. This allows us to obtain directly A_0 and A_1 in the

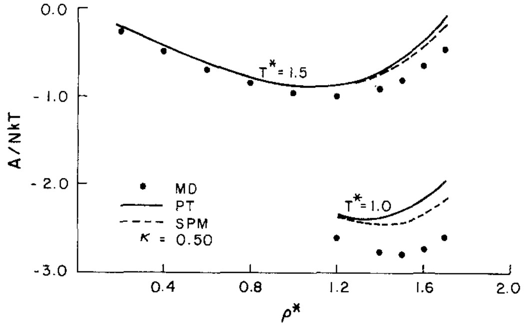

Fig. 1. Comparison of the residual Helmholtz free energy, *A/NkT*, from molecular dynamics (MD), perturbation theory (PT), and the sphericalized potential method (SPM) for the GOCE potential with $\kappa = 0.50$.

perturbation expansion [Eq. (10)] and these terms have been compared with those obtained from perturbation theory [9]. It is found that A_0 from perturbation theory compares well with that from simulation and perturbation theory significantly underpredicts the first-order term A_1. These calculations also show that the first-order expansion (10) itself is a good approximation for the GOCE model and our calculations of A_1 are not sufficiently accurate [9].

Similar studies have also been performed for the GOBG potential with $d_w = 1.0$ and $\kappa = 0.50$ and 1.55 [10]. Figure 2 shows a comparison of the residual Helmholtz free energy from simulation, perturbation theory, and the sphericalized potential method. The improvement in comparison with Fig. 1 for both these methods is significant, especially, for perturbation theory. This is also observed for the case of $\kappa = 1.55$ [10]. As expected, these methods compare well with simulation for pressure and internal energy and also with perturbation theory slightly better than the sphericalized potential method [10]. Table I shows one such comparison for the potential energy.

Simulations using the reference potential have also been performed for the GOBG model and these show A_0 and A_1 from perturbation theory to be in good agreement with simulation for this case [10]. The improvements in the comparison of perturbation theory and the sphericalized potential method with simulation for the GOBG potential over the GOCE model is certainly interesting and we consider this to be due mainly to the use of Eq. (6), which makes the GOBG potential closer to the site–site models for which such methods are already known to work [1].

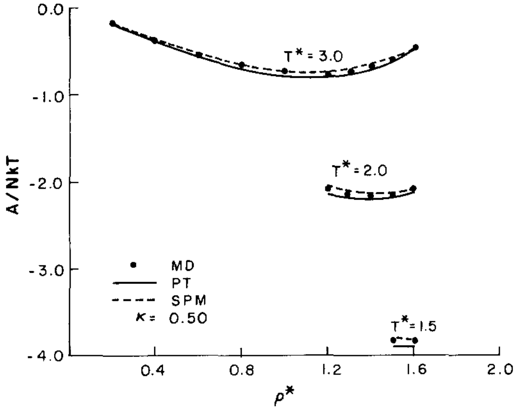

Fig. 2. Same as Fig. 1 for the GOBG potential with $\kappa = 0.50$ and $d_w = 1.0$.

Table I. A Comparison of the Potential Energy from Molecular Dynamics Using the Full Gaussian Overlap Pair Potential (MD—Full) and the Nonspherical Reference Potential (MD—Ref) with Results from Perturbation Theory (PT) and the Sphericalized Potential Method (SPM) for the GOBG Potential (From Ref. 10)

			$U/N\varepsilon_0$			
κ	ρ^*	T^*	*PT*	MD—Ref	MD—Full	SPM
0.50	1.20	3.00	−7.64	−7.55	−7.59	−7.29
		2.00	−8.17	−8.06	−8.13	−7.92
	1.50	3.00	−9.03	−8.86	−8.98	−8.71
		2.00	−9.79	−9.88	−9.78	−9.65
1.55	0.30	1.75	−1.59		−1.68	−1.55
		1.00	−1.83		−1.89	−1.72
	0.50	1.75	−2.54		−2.65	−2.50
		1.00	−3.19		−3.15	−2.95

4. SIMULATION AND EXPERIMENT

Previous studies [8] indicate that the GOBG potential can be used to model liquid benzene, at least for a small range of temperatures, and we have performed such a study on a much wider scale and also included the

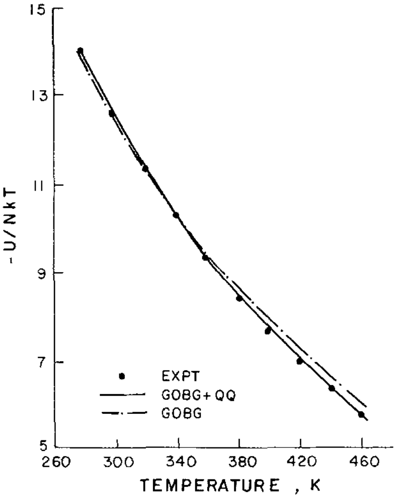

Fig. 3. Comparison of the potential energy of orthobaric liquid benzene from experiment and simulation using the modified Gaussian overlap potential, with (GOBG + QQ) and without (GOBG) the quadrupole moment.

effect of the quadrupole moment. Through systematic NVT simulations, we have obtained zero-pressure liquid densities and potential energies as functions of the temperature for the COBG fluid with $\kappa = 0.50$ and $d_w = 0.58$. For the quadrupolar fluid we used $Q^* = -0.378$ based upon the experimental quadrupole moment [1] and estimated ε_0 and σ_0 [11].

From comparisons of these zero-pressure simulation results with the experimental orthobaric liquid curves we have obtained not only the potential parameters ($\varepsilon_0/\kappa = 483$ K for GOBG and $\varepsilon_0/\kappa = 417$ K for the GOBG + QQ and $\sigma_0 = 6.39$°A for both) but also an idea of how well this potential can model liquid benzene. Figure 3 shows such a comparison for the potential energy. Both the GOBG and the GOBG + QQ models predict well the orthobaric potential energy of liquid benzene, with the quadrupolar potential being slightly better. Figure 4 shows a similar comparison for orthobaric liquid density and here the quadrupolar potential is clearly superior. Figure 5 shows a similar comparison for the second virial coefficient also; there the quadrupolar potential is slightly better. We have also modeled liquid benzene using a six-site potential, with and without the quadrupole moment, and found the COBG potential to be comparable to the six-site potential [11].

The above comparison clearly shows that the Gaussian overlap potential can be used to model real fluids and other systems should be explored. Also, we have so far used only the Lennard–Jones-type expressions such as Eqs. (1) and (6), and other models should also be considered for this purpose. For the present, we are modeling naphthalene as a dumbbell of two oblate ellipsoids using the GOBG potential and the preliminary results are encouraging. The possibility also exists for simulating fluid mixtures.

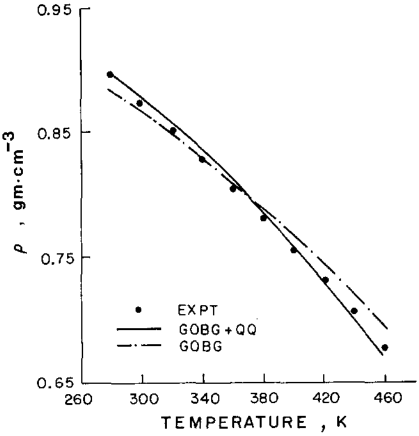

Fig. 4. Same as Fig. 3 for the density.

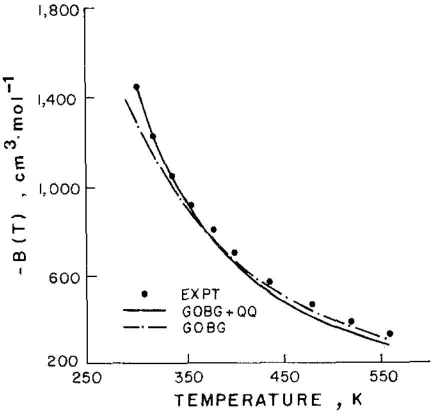

Fig. 5. Comparison of the experimental second virial coefficient for benzene with predictions using the GOBG and GOBG + QQ potentials.

ACKNOWLEDGMENT

This research was supported by Grant DE-FG05-86ER13632 from the Office of Basic Energy Sciences, U.S. Department of Energy.

REFERENCES

1. C. G. Gray and K. E. Gubbins, *Theory of Molecular Fluids, Vol. 1* (Clarendon Press, Oxford, 1984).
2. P. A. Monson and K. E. Gubbins, *J. Phys. Chem.* **87**:2852 (1983).
3. V. R. Bethanabotla and W. Steele, *Mol. Phys.* **60**:249 (1987).
4. B. J. Berne and P. Pechukas, *J. Chem. Phys.* **56**:4213 (1972).
5. J. G. Gay and B. J. Berne, *J. Chem. Phys.* **74**:3316 (1981).
6. J. Kushick and B. J. Berne, *J. Chem. Phys.* **64**:1362 (1976).
7. V. N. Kabadi and W. A. Steele, *Ber. Bunsenges. Phys. Chem.* **89**:2 (1985); **89**:9 (1985).
8. V. N. Kabadi, *Ber. Bunsenges. Phys. Chem.* **90**:327 (1986); **90**:332 (1986).
9. W. B. Sediawan, S. Gupta, and E. McLaughlin, *Mol. Phys.* **62**:141 (1987).
10. W. B. Sediawan, S. Gupta, and E. McLaughlin, *Mol. Phys.* **63**:691 (1988).
11. S. Gupta, W. B. Sediawan, and E. McLaughlin, Submitted for publication (1988).
12. P. S. Y. Cheung, *Chem. Phys. Lett.* **40**:19 (1976).
13. J. Fischer, *J. Chem. Phys.* **72**:5371 (1980).
14. K. C. Mo and K. E. Gubbins, *Chem. Phys. Lett.* **27**:144 (1974).
15. G. O. Williams, J. L. Lebowitz, and J. K. Percus, *J. Chem. Phys.* **81**:2070 (1984).
16. D. MacGowan, E. M. Waisman, J. L. Lebowitz, and J. K. Percus, *J. Chem. Phys.* **80**:2719 (1984).
17. M. S. Shaw, J. D. Johnson, and J. D. Ramshaw, *J. Chem. Phys.* **84**:3479 (1986).
18. B. Kumar, S. Goldman, and W. R. Smith, *J. Chem. Phys.* **84**:6383 (1986).
19. D. McGowan, *J. Chem. Phys.* **81**:3224 (1984).
20. J. A. Barker and D. Henderson, *J. Chem. Phys.* **47**:4714 (1967).